



Communication

Preparation of Large-Size, Superparamagnetic, and Highly Magnetic Fe₃O₄@PDA Core–Shell Submicrosphere-Supported Nano-Palladium Catalyst and Its Application to Aldehyde Preparation through Oxidative Dehydrogenation of Benzyl Alcohols

Haichang Guo ^{1,2}, Renhua Zheng ², Huajiang Jiang ², Zhenyuan Xu ^{1,*} and Aibao Xia ^{1,*}

¹ Zhejiang Key Laboratory of Green Pesticides and Cleaner Production Technology, Catalytic Hydrogenation Research Center, Zhejiang University of Technology, Hangzhou 310014, China; hc.g@163.com

² School of Pharmaceutical and Material Engineering, Taizhou University, Taizhou 318000, China; zhengrh@tzc.edu.cn (R.Z.); jhj@tzc.edu.cn (H.J.)

* Correspondence: greenchem@zjut.edu.cn (Z.X.); xiaaibao@zjut.edu.cn (A.X.); Tel.: +86-571-88320066 (Z.X.); +86-571-88320066 (A.X.)

Received: 30 March 2019; Accepted: 1 May 2019; Published: 3 May 2019



Abstract: Large-size, superparamagnetic, and highly magnetic Fe₃O₄@PDA core–shell submicrosphere-supported nano-palladium catalysts were prepared in this study. Dopamine was encapsulated on the surface of Fe₃O₄ particles via self-polymerization and then protonated to positively charge the microspheres. PdCl₄²⁻ was dispersed on the surface of the microspheres by positive and negative charge attraction and then reduced to nano-palladium. With air as oxidant, the catalyst can successfully catalyze the dehydrogenation of benzyl alcohols to produce the corresponding aldehydes at 120 °C.

Keywords: catalytic dehydrogenation; core–shell structure; dopamine; Fe₃O₄; nano-palladium

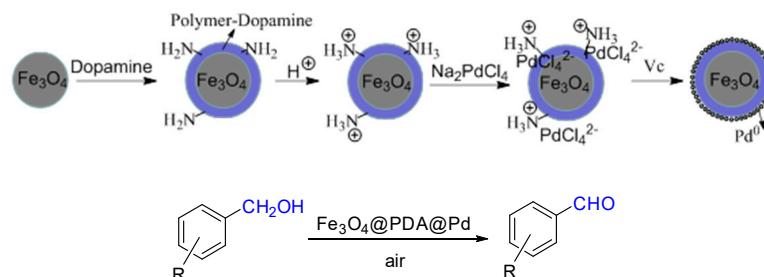
1. Introduction

Fe₃O₄ nanoparticles have been used extensively in many fields due to their superior magnetic properties [1–5] and microwave absorption function [6–9]. Compared with other metal nanoparticles, the preparation of Fe₃O₄ nanoparticles is simple, and the materials used are inexpensive and easily available. Thus, these materials are suitable for industrial production. However, single Fe₃O₄ nanospheres will usually experience an agglomeration phenomenon, which hinders the catalytic reaction. Hence, substances such as SiO₂ [10,11], dopamine [12–15], and surfactant [16–18] are usually used to wrap Fe₃O₄ so that it becomes uniformly dispersed, achieving favorable hydrophilic interactions. This type of Fe₃O₄ with a core–shell structure has enormous application potential in various fields, including bioseparation [19,20], diagnostic analysis [21,22], molecular imprinting [23], and battery energy storage [24]. Moreover, other metal nanoparticles can be introduced on the shell surface, which not only maintains the original high efficiency of other metal catalysts but also has the magnetism of Fe₃O₄. These properties facilitate the separation of catalysts from the reaction mixture.

Benzaldehyde derivative, an important organic chemical raw material, has been widely applied in pesticides [25], medicines [26], spices [27], dyestuff [28], and cosmetics [29]. The preparation of benzaldehyde derivative through catalytic oxidative dehydrogenation is a green synthetic method [30,31]. Magnetic catalysts play a very important role, such as Pd/Fe₃O₄ catalysts, which have been successfully studied. In their catalytic reactions, there is a medium yield of benzaldehyde derivatization under oxygen or air [32], which can be greatly improved by adding equivalent molar alkali as co-catalyst [33–35]. Moreover, a high yield was achieved when peroxide was used as

oxidant [36–38]. Therefore, we focused on the development of a new and efficient $\text{Fe}_3\text{O}_4\text{@PDA@Pd}$ microparticles catalyst for oxidative dehydrogenation of benzyl alcohols without base under air.

To form the $\text{Fe}_3\text{O}_4\text{@PDA}$ core-shell structure, a polydopamine (PDA) layer was wrapped on the surface of large Fe_3O_4 particles through dopamine autoagglutination. The amino group of the microspheres was combined with protons through protonation with positive electricity. PdCl_4^{2-} was dispersed on the surface through positive and negative charge attraction. The large-size, superparamagnetic, and highly magnetic $\text{Fe}_3\text{O}_4\text{@PDA}$ core-shell-submicrosphere-loaded nano-palladium catalyst was prepared through further reduction (Scheme 1). This catalyst was applied in the preparation of aldehyde through oxidative dehydrogenation of benzyl alcohol compounds under air.



Scheme 1. Preparation of $\text{Fe}_3\text{O}_4\text{@PDA@Pd}$ and its catalysis in an oxidative dehydrogenation reaction.

2. Results and Discussion

We characterized and analyzed $\text{Fe}_3\text{O}_4\text{@PDA@Pd}$. As shown in the x-ray diffraction patterns (see Supplementary File), the peaks of Fe_3O_4 and $\text{Fe}_3\text{O}_4\text{@PDA@Pd}$ microparticles were basically identical, that is, they were both characteristic peaks of Fe_3O_4 . $\text{Fe}_3\text{O}_4\text{@PDA@Pd}$ had no characteristic palladium peak, because the palladium particles were very fine under uniform dispersion.

According to the scanning electron microscope (SEM) graph (Figure 1), the particle size of $\text{Fe}_3\text{O}_4\text{@PDA@Pd}$ submicrospheres was within 600–800 nm. Thus, their particle size was large, and nano-palladium particles could be seen in the 100,000 \times SEM graph. During energy-dispersive x-ray spectroscopy (EDS) analysis (Figure 2 and Table 1), the content of palladium weight was 4.24%. In the mapping graph, palladium was uniformly distributed on the surface. According to the mixed weight in the reaction, the theoretical palladium content in $\text{Fe}_3\text{O}_4\text{@PDA@Pd}$ was approximately 2.5%, and the palladium content was measured as 2.3% through inductively coupled plasma atomic emission spectroscopy (ICP-AES). Through EDS analysis, the palladium content was 4.24%, as this analysis is mainly aimed at element composition on the material surface, and palladium particles were distributed on the surface of submicrospheres. Moreover, the measured palladium content was partially high.

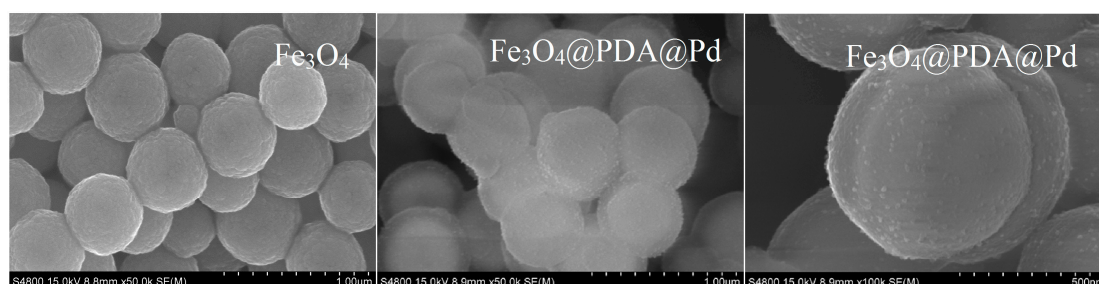
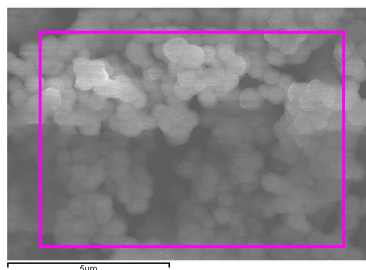
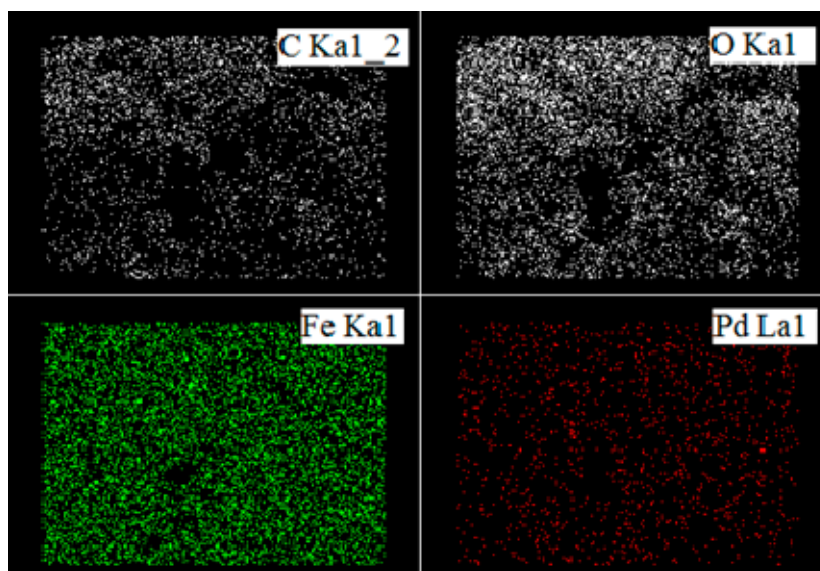


Figure 1. SEM images of Fe_3O_4 and $\text{Fe}_3\text{O}_4\text{@PDA@Pd}$.

Table 1. EDS spectra of Fe₃O₄@PDA@Pd.

Element	wt%
C K	13.43
O K	33.67
Fe K	48.66
Pd L	4.24
Total	100.00

**Figure 2.** Energy-dispersive x-ray spectroscopy (EDS) mapping of Fe₃O₄@PDA@Pd.

The transmission electron microscopy (TEM) graph (Figure 3) shows that the prepared Fe₃O₄@PDA@Pd catalyst presented a core-shell structure that centered on Fe₃O₄ submicrospheres. The dopamine layer was wrapped on the surface of Fe₃O₄ submicrospheres, and the thickness of the shell-layer dopamine was uniformly distributed within the interval of 80–90 nm. Nano-palladium particles were dispersed on dopamine. The palladium (0) particle size was within 7–12 nm, and the average particle size was 9.2 nm.

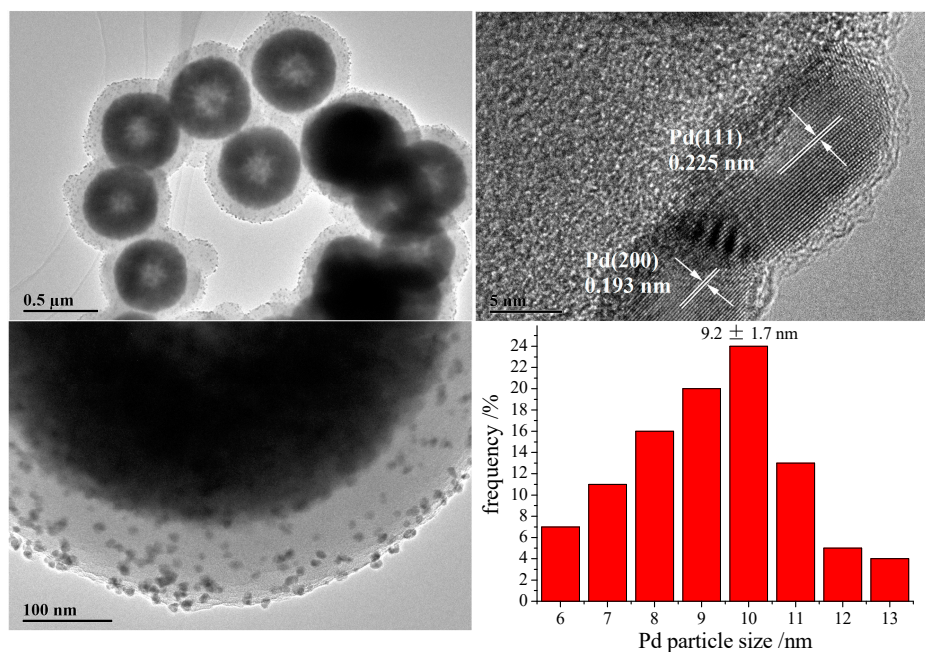


Figure 3. High-resolution transmission electron microscopy (TEM) images of $\text{Fe}_3\text{O}_4@\text{PDA}@\text{Pd}$ and Pd particle size.

Figure 4 shows the magnetization curves of Fe_3O_4 and $\text{Fe}_3\text{O}_4@\text{PDA}@\text{Pd}$ submicrospheres under room temperature (300 K). As shown in the figure, the maximum saturated magnetic intensity of the two submicrospheres was 75 and 45 emu/g, respectively, and the coercive force for both was 0. The existence of the PDA layer decreased the maximum saturated magnetic intensity of $\text{Fe}_3\text{O}_4@\text{PDA}@\text{Pd}$ submicrospheres, but they had superparamagnetic and highly magnetic features. Thus, they could easily disperse and separate from the reaction system.

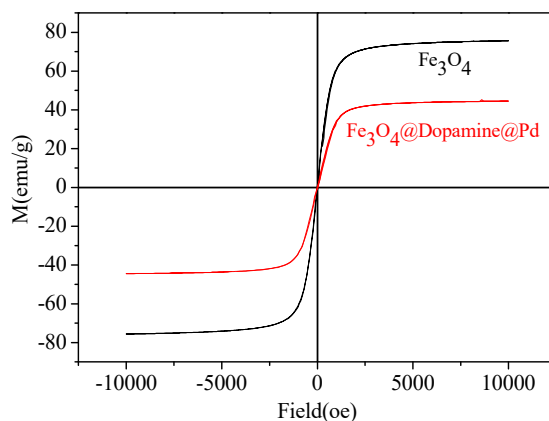


Figure 4. Magnetization curves of Fe_3O_4 and $\text{Fe}_3\text{O}_4@\text{PDA}@\text{Pd}$.

We used $\text{Fe}_3\text{O}_4@\text{PDA}@\text{Pd}$ for aldehyde preparation through oxidative dehydrogenation of benzyl alcohols. The reaction temperature, reaction time, and oxidizing agent for aldehyde preparation through the $\text{Fe}_3\text{O}_4@\text{PDA}@\text{Pd}$ -catalyzed oxidative dehydrogenation of benzyl alcohols were optimized using benzyl alcohol as the substrate (Table 2). The results show that the dehydrogenation reaction did not occur when the reaction temperature was low. The increase in reaction temperature promoted a dehydrogenation reaction. However, when the temperature reached 140 °C, benzyl alcohol products were totally converted, and their selectivity rapidly declined. The product was mainly benzoic acid; hence, the appropriate reaction temperature was 120 °C. Similarly, when the reaction time was too

long, some products were converted into benzoic acids; thus, the appropriate reaction time was 24 h. When oxygen was used as an oxidizing agent, the conversion rate of benzyl alcohols slightly increased, but selectivity declined, indicating that benzaldehyde was easily oxidized under oxygen conditions. Partial benzyl alcohol was converted into benzaldehyde when no oxidizing agent was used, indicating that this catalyst could catalyze benzyl alcohol dehydrogenation even under oxygen-free conditions so as to prepare benzaldehyde. However, the conversion rate was low.

Table 2. Optimization of reaction conditions.

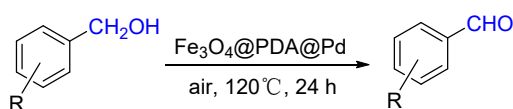


Entry	Temperature (°C)	Time (h)	Oxidant	Conversion ^a (%)	Selectivity ^a (%)
1	80	24	Air	0	–
2	100	24	Air	<5	>99
3	120	12	Air	62	95
4	120	24	Air	80	92
5	120	48	Air	87	79
6	140	24	Air	100	42 ^b
7	120	24	O ₂	86	70
8	120	48	None ^c	31	>99

^a Determined by gas chromatography (GC) using area normalization method; ^b another product (benzoic acid) was 58%; ^c argon protection.

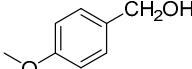
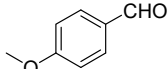
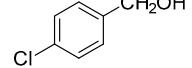
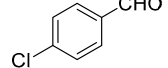
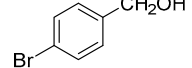
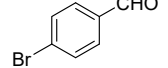
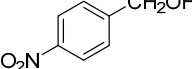
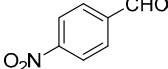
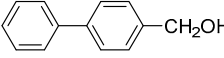
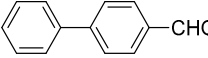
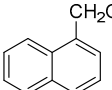
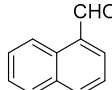
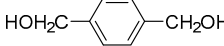

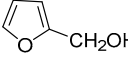
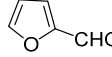
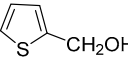
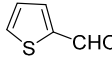
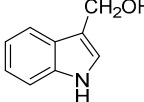
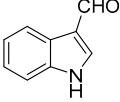
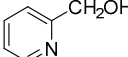
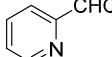
With optimal reaction conditions (Table 2, Entry 4), we checked the reaction scope, and the results are shown in Table 3. There was a medium yield of synthetic aldehyde prepared through Fe₃O₄@PDA@Pd-catalyzed substituent benzyl alcohol dehydrogenation. The dehydrogenation of substituent benzyl alcohols was easier under high-electron cloud density (Entries 2, 3, 4, 8) than under low-electron cloud density (Entries 5, 6, 7). When a substituent group (Entries 1, 9) was present at the adjacent position, it could exert an inhibitory effect on the dehydrogenation reaction of benzyl alcohols, possibly because the existence of adjacent groups affected C–OH bond adsorption by the catalyst. In addition, heterocyclic ring aromatic methanol (Entries 11, 12, 13, 14) could also experience oxidative dehydrogenation to generate the corresponding aldehyde, and a large quantity of acids was generated after 24 h reaction of 2-furancarbinol (Entry 11) and 2-thienylmethanol. All products were characterized by ¹H NMR and ¹³C NMR (see Supplementary File).

Table 3. Catalytic dehydrogenation of substituted benzylic alcohols to aldehydes.



Entry	Substituted Benzylic Alcohol	Aldehyde	Yield ^a (%)
1			57
2			76
3			77

Table 3. Cont.

Entry	Substituted Benzylic Alcohol	Aldehyde	Yield ^a (%)
4			84
5			73
6			71
7			60
8			86
9			69
10			53
11			65 ^b
12			72 ^b
13			72
14			74

^a Isolated yield; ^b 12 h.

Fe₃O₄@PDA@Pd permits easy recovery of the catalyst from the reaction mixture by a magnet. The reusability of the recovered catalyst was evaluated for the oxidative dehydrogenation of benzyl alcohol as a model reaction, and nearly 95% of its original activity was retained even after five cycles (Figure 5). After six cycles, its activity decreased but its catalytic selectivity remained almost invariant. Compared with the fresh catalysts by SEM and EDS (see Supplementary File), we found that the catalysts were partially fractured and the palladium content was reduced by nearly half.

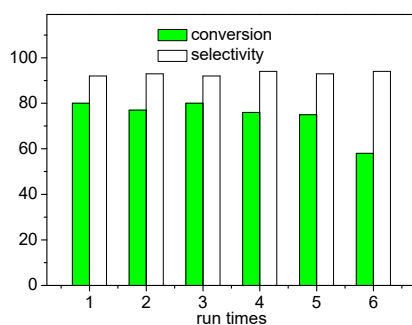


Figure 5. Recycling of the $\text{Fe}_3\text{O}_4@\text{PDA}@\text{Pd}$ catalyst in oxidative dehydrogenation of benzyl alcohol.

3. Materials and Methods

Commercially available reagents were used without further purification. The x-ray diffraction (XRD) analysis used a Bruker AXS D8 Advance diffractometer. Scanning electron microscope (SEM) and energy-dispersive spectrometry (EDS) images were recorded on a Hitachi S-4800 field emission scanning electron microscope equipped with an energy-dispersive spectrometer. Transmission electron microscopy (TEM) images were obtained on a JEOL JEM-2100F field transmission electron microscope. Magnetic information was obtained on a Quantum Design DynaCool-9 vibrating sample magnetometer. The ^1H NMR and ^{13}C NMR spectra were recorded on a Bruker Avance 400 MHz spectrometer using tetramethylsilane (TMS) as internal standard.

Fe_3O_4 particles were prepared according to the method specified in Reference [39].

The general procedure was for the preparation of $\text{Fe}_3\text{O}_4@\text{PDA}$. Approximately 0.15 g of strong ammonia water was dissolved in 50 mL of deionized water. Then, 0.1 g of Fe_3O_4 and 0.16 g of dopamine hydrochloride were added, and the mixture was placed under uniform ultrasonic dispersion and mechanical agitation under 40 °C for 24 h. After the reaction ended, solid and liquor were separated using a magnet. The product was placed under ultrasonic washing using 25 mL \times 3 deionized water and 25 mL \times 3 ethanol, and the solid was directly used in the next step.

The general procedure for the preparation of $\text{Fe}_3\text{O}_4@\text{PDA}@\text{Pd}$ was as follows. To prepare palladium sodium chloride solution, 0.115 g (approximately 0.65 mmol) of palladium chloride and 0.076 g (approximately 1.3 mmol) of sodium chloride were taken, and deionized water was added dropwise until the weight reached 8 g. The mixture was heated to 50 °C, and a palladium sodium chloride solution was prepared and placed in a brown bottle for later use. To prepare $\text{Fe}_3\text{O}_4@\text{PDA}$ -loaded nano-palladium, $\text{Fe}_3\text{O}_4@\text{PDA}$ solid was placed under ultrasonic washing using 25 mL of deionized water, 0.1 N of 25 mL hydrochloric acid, 25 mL of deionized water, and 25 mL of ethanol. Approximately 40 mL of ethanol and 4 mL of deionized water were added, and the mixture was mechanically agitated under 10 °C. Subsequently, 0.29 g of palladium sodium chloride solution was slowly added dropwise, and then the mixture was continuously agitated for 3 h. A solution comprising 60 mg of ascorbic acid and 6 mL of deionized water was added slowly using a needle cylinder for 20 min. Afterward, the reaction lasted for 2 h. The solid and liquor were separated using a magnet; the reaction product was placed under ultrasonic washing using 25 mL of ethanol, 25 mL \times 3 deionized water, and 25 mL \times 3 ethanol. The solid was preserved in 25 mL of ethanol and sealed using nitrogen (solid was approximately 0.1 g after drying).

The general procedure for the oxidative dehydrogenation of benzyl alcohol was as follows. Approximately 0.1 g of $\text{Fe}_3\text{O}_4@\text{PDA}@\text{Pd}$ catalyst (2 mol% of Pd) was used. The aforementioned solid and liquor were separated using a magnet and placed under ultrasonic washing using 10 mL \times 3 O-xylene. Then, 1 mmol of benzyl alcohol derivative and 5 mL of O-xylene were successively added and blended under ultrasonic conditions. The mixture was then magnetically stirred for 24 h under 120 °C. After the reaction ended, the solid and liquor were separated using a magnet. The liquor was concentrated, and the dehydrogenation product could be obtained after purification through column chromatography (petroleum ether/ethyl acetate).

4. Conclusions

We developed a method for preparing large-size, superparamagnetic, and highly magnetic Fe₃O₄@PDA core-shell submicrosphere-supported nano-palladium catalysts. The catalysts could catalyze the dehydrogenation of benzyl alcohols to produce the corresponding aldehydes with medium to high yields under air as oxidant without base. Additionally, they could be easily removed from the reaction media by an external magnet and reused five times without a considerable reduction in reactivity.

Supplementary Materials: The supplementary materials are available online.

Author Contributions: H.G., Z.X., and A.X. conceived and designed the experiments; H.G. and R.Z. performed the experiments; H.G. and H.J. analyzed the data; H.J., Z.X., and A.X. contributed the reagent/material/analysis tools; H.G. wrote the paper. All authors have read the final version of the manuscript.

Funding: We thank the Zhejiang Province Public Welfare Technology Research Program (LGG19B040001), Zhejiang Natural Science Foundation (LY18B020017), and Taizhou Science and Technology Project (1801gy21) for their financial support.

Conflicts of Interest: The authors declare no conflict of interest.

References

1. Xu, H.; Cui, L.L.; Tong, N.H.; Gu, H.C. Development of high magnetization Fe₃O₄/polystyrene/silica nanospheres via combined miniemulsion/emulsion polymerization. *J. Am. Chem. Soc.* **2006**, *128*, 15582–15583. [[CrossRef](#)]
2. Lima, E.; Brandl, A.L.; Arelaro, A.D.; Goya, G.F. Spin disorder and magnetic anisotropy in Fe₃O₄ nanoparticles. *J. Appl. Phys.* **2006**, *99*, 083908. [[CrossRef](#)]
3. Allia, P.; Barrera, G.; Tiberto, P.; Nardi, T.; Leterrier, Y.; Sangermano, M. Fe₃O₄ nanoparticles and nanocomposites with potential application in biomedicine and in communication technologies: Nanoparticle aggregation, interaction, and effective magnetic anisotropy. *J. Appl. Phys.* **2014**, *116*, 113903. [[CrossRef](#)]
4. Li, G.Z.; Wang, X.Q.; Row, H.K. Magnetic solid-phase extraction with Fe₃O₄/molecularly imprinted polymers modified by deep eutectic solvents and ionic liquids for the rapid purification of alkaloid isomers (theobromine and theophylline) from green tea. *Molecules* **2017**, *22*, 1061. [[CrossRef](#)] [[PubMed](#)]
5. Devi, S.M.; Nivetha, A.; Prabha, I. Superparamagnetic Properties and Significant Applications of Iron Oxide Nanoparticles for Astonishing Efficacy—a Review. *J. Supercond. Nov. Magn.* **2018**, *3*, 1–18. [[CrossRef](#)]
6. Peelamedu, R.; Grimes, C.; Cheng, J.; Agrawal, D. Major phase transformations and magnetic property changes caused by electromagnetic fields at microwave frequencies. *J. Mater. Res.* **2002**, *17*, 3008–3011.
7. Qiang, C.; Xu, J.; Zhang, Z.; Tian, L.; Xiao, S.; Liu, Y.; Xu, P. Magnetic properties and microwave absorption properties of carbon fibers coated by Fe₃O₄ nanoparticles. *J. Alloys Compd.* **2010**, *506*, 93–97. [[CrossRef](#)]
8. Mordina, B.; Kumar, R.; Tiwari, R.K.; Setua, D.K.; Sharma, A. Fe₃O₄ Nanoparticles Embedded Hollow Mesoporous Carbon Nanofibers and Polydimethylsiloxane-Based Nanocomposites as Efficient Microwave Absorber. *J. Phys. Chem. C* **2017**, *121*, 7810–7820. [[CrossRef](#)]
9. Zhang, K.; Gao, X.; Zhang, Q.; Chen, H.; Chen, X. Fe₃O₄ nanoparticles decorated MWCNTs @ C ferrite nanocomposites and their enhanced microwave absorption properties. *J. Magn. Magn. Mater.* **2018**, *452*, 55–63. [[CrossRef](#)]
10. Tartaj, P.; Serna, C.J. Synthesis of monodisperse superparamagnetic Fe/silica nanospherical composites. *J. Am. Chem. Soc.* **2003**, *125*, 15754–15755. [[PubMed](#)]
11. Khosroshahi, M.E.; Ghazanfari, L. Amino surface modification of Fe₃O₄/SiO₂ nanoparticles for bioengineering applications. *Surf. Eng.* **2013**, *27*, 508–573. [[CrossRef](#)]
12. Ding, C.F.; Sun, Y.L.; Wang, Y.H.; Li, J.B.; Lin, Y.N.; Sun, W.Y.; Luo, C.N. Adsorbent for resorcinol removal based on cellulose functionalized with magnetic poly(dopamine). *Int. J. Biol. Macromol.* **2017**, *99*, 578–585. [[CrossRef](#)] [[PubMed](#)]
13. Chattopadhyay, T.; Chakraborty, A.; Dasgupta, S.; Dutta, A.; Menéndez, M.I.; Zangrando, E. A route to magnetically separable nanocatalysts: Combined experimental and theoretical investigation of alkyl substituent role in ligand backbone towards epoxidation ability. *Appl. Organomet. Chem.* **2016**, *31*, e3663. [[CrossRef](#)]

14. Dam, B.; Patil, R.A.; Ma, Y.; Pal, A.K. Preparation, characterization and catalytic application of nano-Fe₃O₄-DOPA-SnO₂ having high TON and TOF for non-toxic and sustainable synthesis of dihydroquinazolinone derivatives. *New J. Chem.* **2017**, *41*, 6553–6563. [[CrossRef](#)]
15. Gao, F.; Qu, H.; Duan, Y.Y.; Wang, J.; Song, X.; Ji, T.J.; Cao, L.X.; Nie, G.G.; Sun, S.G. Dopamine coating as a general and facile route to biofunctionalization of superparamagnetic Fe₃O₄ nanoparticles for magnetic separation of proteins. *RSC Adv.* **2014**, *4*, 6657–6663. [[CrossRef](#)]
16. Li, X.N.; Wen, F.; Creran, B.; Jeong, Y.; Zhang, X.R.; Rotello, V.M. Colorimetric protein sensing using catalytically amplified sensor arrays. *Small* **2012**, *8*, 3589–3592. [[CrossRef](#)] [[PubMed](#)]
17. Li, X.M.; Si, H.L.; Niu, J.Z.; Shen, H.B.; Zhou, C.G.; Yuan, H. Size-controlled syntheses and hydrophilic surface modification of Fe₃O₄, Ag, and Fe₃O₄/Ag heterodimer nanocrystals. *Dalton Trans.* **2010**, *39*, 10984–10989. [[CrossRef](#)] [[PubMed](#)]
18. Harris, R.A.; Vand, W.H.; Shumbula, P.M. Engineered Inorganic/Organic-Core/Shell Magnetic Fe₃O₄ Nanoparticles with Oleic Acid and/or Oleylamine As Capping Agents. *Curr. Pharm. Des.* **2015**, *21*, 5369–5388. [[CrossRef](#)]
19. Bagga, K.; Brougham, D.F.; Keyes, T.E.; Brabazon, D. Magnetic and noble metal nanocomposites for separation and optical detection of biological species. *Phys. Chem. Chem. Phys.* **2015**, *17*, 27968–27980. [[CrossRef](#)]
20. Batalha, Í.L.; Roque, A.C. Phosphopeptide Enrichment Using Various Magnetic Nanocomposites: An Overview. *Methods Mol. Biol.* **2016**, *1355*, 193–209.
21. Gujrati, V.; Mishra, A.; Ntziachristos, V. Molecular imaging probes for multi-spectral optoacoustic tomography. *Chem. Commun.* **2017**, *53*, 4653–4672. [[CrossRef](#)]
22. Li, J.C.; Wang, S.G.; Shi, X.Y.; Shen, M.W. Aqueous-phase synthesis of iron oxide nanoparticles and composites for cancer diagnosis and therapy. *Adv. Colloid Interface Sci.* **2017**, *249*, 374–385. [[CrossRef](#)]
23. Wu, M.; Deng, H.Y.; Fan, Y.J.; Hu, Y.C. Rapid Colorimetric Detection of Cartap Residues by AgNP Sensor with Magnetic Molecularly Imprinted Microspheres as Recognition Elements. *Molecules* **2018**, *23*, 1443. [[CrossRef](#)]
24. Wang, L.; Yue, S.Y.; Zhang, Q.; Zhang, Y.M. Morphological and Chemical Tuning of High-Energy-Density Metal Oxides for Lithium Ion Battery Electrode Applications. *ACS Energy Lett.* **2017**, *2*, 1465–1478. [[CrossRef](#)]
25. Schacht, E.; Desmarests, G.; Bogaert, Y. Polymeric pesticides, 4. Synthesis of polyamides and a polyester containing 2,6-dichlorobenzaldehyde. *Macromol. Chem. Phys.* **1978**, *179*, 837–840. [[CrossRef](#)]
26. Derya, O.; Serkan, L.; Abdullah, B.K.; Sinem, I. Synthesis of New Benzothiazole Acylhydrazones as Anticancer Agents. *Molecules* **2018**, *23*, 1054.
27. Chen, J.J.; Lin, Y.H.; Day, S.H.; Hwang, T.L.; Chen, I.S. New benzenoids and anti-inflammatory constituents from *Zanthoxylum nitidum*. *Food Chem.* **2011**, *125*, 282–287. [[CrossRef](#)]
28. Bello, K.A.; Martins, C.M.O.A.; Adamu, I.K. Methine dyes formed by condensation of indane-1,3-dione and cyanovinyl analogues with benzaldehydes. *Color. Technol.* **2010**, *110*, 238–240.
29. Young, Y.H.; Hyun, K.D.; Sujin, S.; Sultan, U.; Jin, K.; Young, Y.; Ryong, M.H. Design, synthesis, and anti-melanogenic effects of (E)-2-benzoyl-3-(substituted phenyl)acrylonitriles. *Drug Des. Dev. Ther.* **2015**, *9*, 4259–4268.
30. Kopylovich, M.N.; Ribeiro, A.P.C.; Alegria, E.C.B.A.; Martins, N.M.R.; Martins, L.M.D.R.S.; Pombeiro, A.J.L. Catalytic Oxidation of Alcohols: Recent Advances. *ChemInform* **2016**, *47*, 91–174. [[CrossRef](#)]
31. Majumdar, B.; Sarma, D.; Jain, S.; Sarma, T.K. One-Pot Magnetic Iron Oxide-Carbon Nanodot Composite Catalyzed Cyclooxidative Aqueous Tandem Synthesis of Quinazolinones in the Presence of tert-Butyl Hydroperoxide. *ACS Omega* **2018**, *3*, 13711–13719. [[CrossRef](#)]
32. Zamani, F.; Hosseini, S.M. Palladium nanoparticles supported on Fe₃O₄/amino acid nanocomposite: Highly active magnetic catalyst for solvent-free aerobic oxidation of alcohols. *Catal. Commun.* **2014**, *43*, 164–168. [[CrossRef](#)]
33. Dadras, A.; Naimi-Jamal, M.R.; Moghaddam, F.M.; Ayati, S.E. Green and selective oxidation of alcohols by immobilized Pd onto triazole functionalized Fe₃O₄ magnetic nanoparticles. *J. Chem. Sci.* **2018**, *130*, 162. [[CrossRef](#)]
34. Zohreh, N.; Hosseini, S.H.; Tavakolizadeh, M.; Busuioc, C.; Negrea, R. Palladium pincer complex incorporation onto the Fe₃O₄-entrapped crosslinked multilayered polymer as a high loaded nanocatalyst for oxidation. *J. Mol. Liq.* **2018**, *266*, 393–404. [[CrossRef](#)]

35. Movahed, S.K.; Lehi, N.F.; Dabiri, M. Palladium nanoparticles supported on core-shell and yolk-shell Fe_3O_4 @nitrogen doped carbon cubes as a highly efficient, magnetically separable catalyst for the reduction of nitroarenes and the oxidation of alcohols. *J. Catal.* **2018**, *364*, 69–79. [[CrossRef](#)]
36. Ramazani, A.; Khoobi, M.; Sadri, F.; Tarasi, R.; Shafiee, A.; Aghahosseini, H.; Joo, S.W. Efficient and selective oxidation of alcohols in water employing palladium supported nanomagnetic Fe_3O_4 @hyperbranched polyethylenimine (Fe_3O_4 @HPEI.Pd) as a new organic-inorganic hybrid nanocatalyst. *Appl. Organomet. Chem.* **2018**, *32*, e3908. [[CrossRef](#)]
37. Baig, R.B.N.; Nadagouda, M.N.; Varma, R.S. Carbon-coated magnetic palladium: Applications in partial oxidation of alcohols and coupling reactions. *Green Chem.* **2014**, *16*, 4333–4338. [[CrossRef](#)]
38. Shokouhimehr, M.; Shin, K.Y.; Lee, J.S.; Hackett, M.J.; Jun, S.W.; Oh, M.H.; Jang, J.; Hyeon, T. Magnetically recyclable core-shell nanocatalysts for efficient heterogeneous oxidation of alcohols. *J. Mater. Chem. A* **2014**, *2*, 7593–7599. [[CrossRef](#)]
39. Deng, H.; Li, X.L.; Peng, Q.; Wang, X.; Chen, J.P.; Li, Y.D. Monodisperse magnetic single-crystal ferrite microspheres. *Angew. Chem. Int. Ed.* **2005**, *44*, 2782–2785. [[CrossRef](#)]

Sample Availability: Samples of the compounds Fe_3O_4 , 4-methoxybenzaldehyde, 4-chlorobenzaldehyde and 4-biphenylcarboxaldehyde are available from the authors.



© 2019 by the authors. Licensee MDPI, Basel, Switzerland. This article is an open access article distributed under the terms and conditions of the Creative Commons Attribution (CC BY) license (<http://creativecommons.org/licenses/by/4.0/>).